Respiratory Physiology & Neurobiology 173 (2010) 230–243

Contents lists available at ScienceDirect

Respiratory Physiology & Neurobiology

journal homepage: www.elsevier.com/locate/resphysiol

Review

The role of the central chemoreceptors: A modeling perspective☆

James Duffin[a,b,*]

[a] Departments of Physiology & Anaesthesia, University of Toronto, 1 King's College Circle, Toronto, ON, Canada, M5S 1A8
[b] Thornhill Research, 210 Dundas Street West, Suite 200, Toronto, ON, Canada, M5G 2E8

ARTICLE INFO

Article history:
Accepted 8 March 2010

Keywords:
Respiration
Chemoreflexes
Modeling

ABSTRACT

After introducing the respiratory control system, a previously developed model of the respiratory chemoreflexes, based on rebreathing test data, is briefly described. This model is used to gain insights into the respiratory chemoreflex characteristics of a selection of individuals, and so discover the role of their central chemoreceptors. The chemoreflex model characteristics for each individual were estimated by adjusting the model parameters so that its predictions fit their rebreathing test results. To gain a steady state description of the control of breathing at rest the chemoreflex model is combined with a model of the cerebrovascular reactivity and converted from P_{CO_2} to $[H^+]$ chemoreceptor inputs. This description is used to illustrate how acid–base and cerebrovascular reactivity factors affect the environment of the central chemoreceptors and determine their role in breathing control. Finally, a dynamic model incorporating the chemoreflex model, acid–base and cerebrovascular reactivity is used to show the role of the central chemoreceptors in stabilizing breathing during sleep at altitude.

1. Introduction

Models of the chemoreflex control of breathing have been constructed for many years and recent examples include both steady state (Duffin et al., 2000; Stephenson, 2004; Duffin, 2005; Duffin, 2007) and dynamic versions (Ursino and Magosso, 2004; Stuhmiller and Stuhmiller, 2005; Topor et al., 2007; Wolf and Garner, 2007; Zhou et al., 2007; Longobardo et al., 2008). The models are used to elucidate the operation of the respiratory control system under a variety of circumstances, and here I use a model of the respiratory chemoreflexes to illustrate the role of the central chemoreceptors in the control of breathing. After a brief review of the physiology of the respiratory chemoreflexes, I describe a previously developed model, whose parameters are based on experimental measurements made using modified rebreathing tests (Duffin et al., 2000).

Then, to discover the roles of the central and peripheral chemoreceptors and how they vary among individuals, I examine data from modified rebreathing tests of selected individuals. Adjusting the chemoreflex model parameters until the model prediction matches the rebreathing responses observed yields estimates of the chemoreflex characteristics of these individuals, and these show the role played by the central chemoreceptors in regulating their resting breathing.

Following this examination of the chemoreflexes, I describe the incorporation of the chemoreflex model into both steady state and dynamic models of the respiratory control system. This process involves including models of the control of cerebral blood flow and acid–base balance; factors that affect the central chemoreceptor tissue environment, and hence, the stimulus to the central chemoreceptors. The steady state model illustrates the interaction of the cerebrovascular reactivity to CO_2 and the respiratory chemoreflexes in the control of breathing (Ainslie & Duffin, 2009). The dynamic model shows how central chemoreceptors stabilize breathing during sleep at altitude and the effects of cerebrovascular reactivity.

2. The respiratory control system

Breathing is regulated by two anatomically distinct but functionally integrated systems; the metabolic (automatic) and the behavioral (voluntary) respiratory control systems. The metabolic system regulates acid–base balance and blood gas homeostasis, receiving afferent information from peripheral and central chemoreceptors sensitive to $[H^+]$ and P_{O_2}, and from bronchopulmonary mechanoreceptors sensitive to the degree of lung stretch and rate of airflow. In contrast, the behavioral control system uses the breathing apparatus for functions whose primary purpose is not gas exchange, for example, speaking. It is the former system that is of concern here and Fig. 1 shows a crude compartment model of the body and the location of the respiratory chemoreceptors. The

☆ This paper is part of a special issue entitled "Central Chemoreception", guest-edited by Drs. E.E., Nattie and H.V. Forster.

* Correspondence address: Thornhill Research, 210 Dundas Street West, Suite 200, Toronto, ON, Canada, M5G 2E8. Tel.: +1 416 597 1325x291; fax: +1 416 978 4940.
E-mail address: j.duffin@utoronto.ca.

1569-9048/$ – see front matter © 2010 Elsevier B.V. All rights reserved.
doi:10.1016/j.resp.2010.03.010

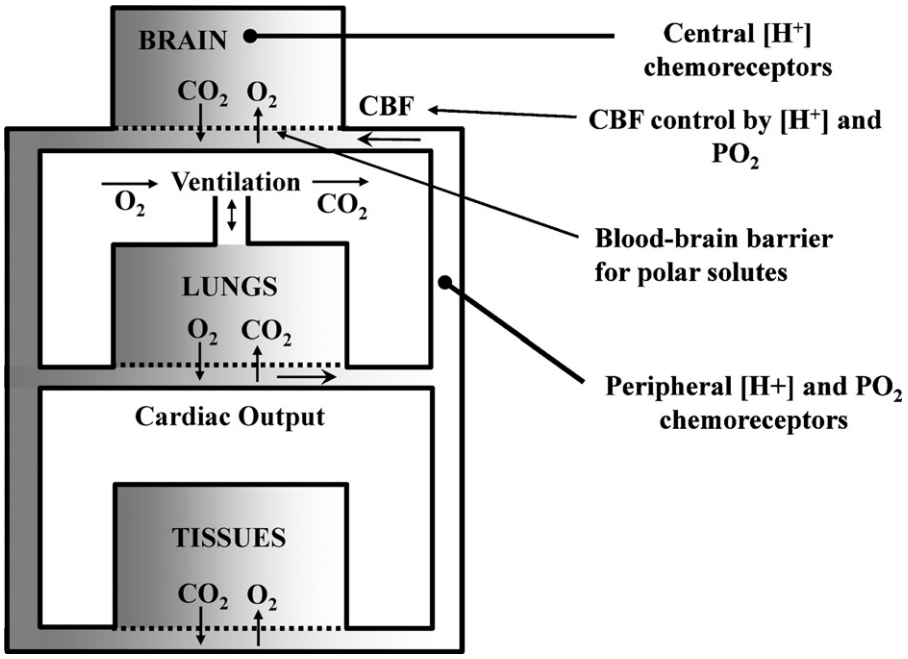

Fig. 1. A simple three-compartment model of gas exchange. The locations of the central and peripheral chemoreceptors are shown. The lung compartment models the pulmonary gas exchange with the blood passing through it as well as the ventilation controlled gas exchange with the environment. The brain compartment models the medullary tissues where the central chemoreceptors are located, and the tissue compartment represents the rest of the body tissues. Cardiac output circulates blood from the lung compartment to the brain and tissues compartments. The brain tissue compartment is protected from systemic acid–base disturbances by the blood–brain barrier for polar solutes, and the control of cerebral blood flow (CBF) mitigates systemic P_{CO_2} disturbances.

compartments are separated into O_2 and CO_2 sub compartments with the CO_2 compartments much larger than the O_2 because CO_2 is stored in tissue water whereas O_2 is stored mostly in blood. These different compartment sizes determine their rates of gas equilibration with the blood in dynamic situations so that P_{O_2} changes much faster than P_{CO_2}.

The metabolic control system is responsible for providing O_2 for metabolism and eliminating the CO_2 produced by metabolism. It accomplishes this goal by adjusting pulmonary ventilation so that O_2 uptake via the lungs equals O_2 consumption by the tissues, and CO_2 elimination at the lungs equals CO_2 production by the tissues. Under these conditions, where pulmonary gas exchange matches metabolism, P_{O_2} and P_{CO_2} remain constant. Their values must satisfy the following physiological requirements.

The requirement for P_{O_2} is relatively simple; it should be sufficient to saturate arterial hemoglobin, and maintain a pressure gradient capable of supplying O_2 to the tissues. Because of the shape of the hemoglobin dissociation curve, saturation occurs over a wide range of P_{O_2}, and so P_{O_2} need not be closely regulated, as long as tissue hypoxia is avoided.

The requirement for P_{CO_2} differs. CO_2 elimination is less dependent on a pressure gradient because CO_2 diffuses through aqueous membranes much more readily than O_2. However, P_{CO_2} must be controlled to ensure that tissue $[H^+]$ remains within the narrow limits necessary for optimal protein function, especially in the brain (Nattie, 1990). This requirement for the brain is so important that ionic concentrations affecting acid–base balance are also regulated as well as cerebral blood flow.

The respiratory chemoreflex control system ensures that these requirements are met using inputs from two chemoreceptors that sense $[H^+]$, one in the brain (central chemoreceptors) and one in the carotid bodies (peripheral chemoreceptors). These chemoreceptors respond such that when $[H^+]$ increases, breathing is stimulated, so that under resting conditions, P_{CO_2} is maintained within a narrow range. Protection against asphyxia is provided by the peripheral chemoreceptors that increase their sensitivity to $[H^+]$ under conditions of hypoxia. Ignored in the models described here is the response to an increase in metabolism by exercise, which must be accompanied by increased breathing if pulmonary gas exchange is to match metabolism. In this situation, fast neural response mechanisms are activated, including afferent feedback from the exercising muscles and a parallel activation of ventilation and the exercising muscles (Mateika and Duffin, 1995; Bell, 2006).

3. The chemoreflex model

3.1. General organization

The chemoreflex control of breathing shown schematically in Fig. 2 is a negative feedback loop based on the control of $[H^+]$. An increase in $[H^+]$ stimulates an increase in breathing, which reduces P_{CO_2} and consequently $[H^+]$; hence the negative feedback designation of the system.

The forward part of the loop describes the effect pulmonary gas exchange has on P_{CO_2} and P_{O_2} and can be characterized by the relationships between ventilation and P_{CO_2} and P_{O_2}. In this case P_{CO_2} is the major factor controlling the $[H^+]$ sensed by the chemoreceptors, and so we concentrate on that relationship. Assuming no CO_2 is inspired, the product of alveolar ventilation and alveolar P_{CO_2} is proportional to the amount of carbon dioxide eliminated, so that in any steady state, P_{CO_2} depends on CO_2 production divided by alveolar ventilation. This equation describes a rectangular hyperbola and is called the iso-metabolic hyperbola.

The feedback part of the loop is the control of pulmonary ventilation in response to changes in P_{CO_2}, which alter $[H^+]$, and P_{O_2}, at the chemoreceptors. The transition from a chemoreceptor stimulus to alveolar ventilation occurs via a pathway that includes the chemoreceptors that sense the signal, the central nervous system that processes it, and the respiratory muscles that translate it into alveolar ventilation. The pathway and process is termed a chemoreflex. In addition to chemoreflex drives to breathing, an independent drive to breathe also contributes to ventilation that reflects the

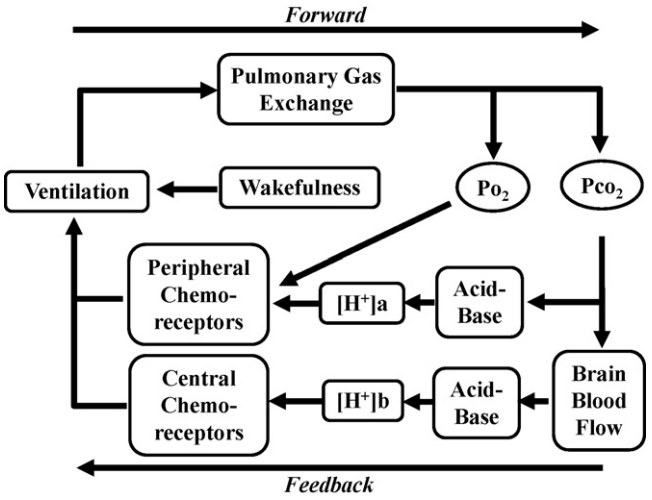

Fig. 2. A block diagram showing the major elements in the chemoreflex control of breathing. Ventilation controls P_{CO_2} and P_{O_2} via the gas exchange in the lungs (the forward part of the control loop). P_{CO_2} controls brain blood flow, as well as central and peripheral [H^+] via acid–base relationships. Central and peripheral chemoreceptors drive ventilation according to the levels of P_{O_2} and [H^+] to form a chemoreflex (the feedback part of the control loop). The control system is termed negative feedback because an increase in ventilation decreases P_{CO_2}, which in turn decreases the chemoreceptors feedback driving ventilation. Note that "other" drives to breathe, such as wakefulness, behavior and exercise, also affect ventilation.

"state" of the subject, and is referred to as the "wakefulness drive," because it is withdrawn during sleep (Fink, 1961; Shea, 1996; Orem et al., 2002). These drives constitute the feedback part of the loop. There are two chemoreflexes, central and peripheral, which are defined by the location of their sensors.

3.2. Central chemoreflex

The central chemoreceptors respond to the [H^+] of their local environment and are often thought of as CO_2 receptors because central [H^+] is directly dependent on the P_{CO_2}, but it should be kept in mind that other independent acid–base factors determine the relationship between [H^+] and P_{CO_2}. The central chemoreceptors are located in the medulla in a number of possible locations; near the ventrolateral surface (Okada et al., 2002) and scattered within the brain tissue (Nattie and Li, 2009), within the retrotrapezoid nucleus (Guyenet et al., 2009), within the Raphe (Corcoran et al., 2009) and within the locus ceruleus (Putnam et al., 2004).

Two factors complicate the physiology of the central chemoreceptors. First, the blood–brain barrier to polar solutes prevents changes in arterial [H^+] from reaching the central chemoreceptors, whereas CO_2 passes freely across the barrier. As a result, central [H^+] may differ from arterial [H^+], isolating the central chemoreceptors from arterial acid–base disturbances, except as they involve changes in arterial P_{CO_2}.

Second, the stimulus to the central chemoreceptors is the [H^+] of medullary brain tissue, which is determined by medullary tissue P_{CO_2} and other independent acid–base factors. Medullary tissue P_{CO_2} is determined by three factors; the arterial P_{CO_2}, the CO_2 production of medullary tissue and the medullary blood flow. Central chemoreceptor P_{CO_2} therefore varies directly with arterial P_{CO_2} and inversely with medullary blood flow for any constant brain metabolic state. Moreover, the medullary tissue P_{CO_2} responds slowly to P_{CO_2} changes in arterial blood, the time constant for the central chemoreceptor response to a change in alveolar P_{CO_2} is about 100 s (Farhi and Rahn, 1960). It therefore it takes about 5 min (three time constants) for the central chemoreceptor stimulus to catch up to changes in inspired CO_2.

3.3. Peripheral chemoreflex

The peripheral chemoreceptors, located in the carotid bodies at the bifurcation of the carotid arteries, respond to the [H^+] and P_{O_2} of the blood approaching the brain. Signals from the receptors are sent to the respiratory controller in the medulla via the carotid sinus nerve (a branch of the glossopharyngeal or IXth cranial nerve) (Iturriaga et al., 2007; Kumar, 2007; Lopez-Barneo et al., 2009). Hypoxia's primary role is to increase the sensitivity of the peripheral chemoreceptors to arterial [H^+] (Mohan and Duffin, 1997). This feature of the peripheral chemoreceptors has two important implications: if the P_{O_2} is high, there is little (if any) peripherally-mediated ventilatory response to P_{CO_2}; and if P_{CO_2} is below the ventilatory recruitment threshold, there is little (if any) response to hypoxia (Jounieaux et al., 2002). These receptors are therefore maximally stimulated by a simultaneous increase in [H^+] and decrease in P_{O_2} i.e. by asphyxia (Torrance, 1996). The peripheral chemoreceptors also transmit a tonic activity (Dahan et al., 2007), which has been hypothesized to increase during hypoxia in chronic exposures (Duffin and Mahamed, 2003) and to be present in some individuals.

3.4. Chemoreflex parameter measurement

Ideally the input–output relationships for a model of the chemoreflexes would be determined by measuring the chemoreceptor inputs of [H^+] and arterial P_{O_2} and the resulting ventilation as shown in Fig. 2. Such measurements cannot be made non-invasively and so indirect measurements are substituted. Instead of [H^+], P_{CO_2} is measured, with end-tidal P_{CO_2} and P_{O_2} as reasonably good estimates of arterial P_{CO_2} and P_{O_2} in healthy young individuals.

Although the inputs to the peripheral chemoreceptors can be considered to be measured by end-tidal P_{CO_2} and P_{O_2}, central P_{CO_2}, the input to the central chemoreceptors, cannot. However, Read (1967) described a rebreathing method to overcome this difficulty. Individuals rebreathe from a small bag, which at the start of rebreathing contains enough CO_2 to equilibrate the P_{CO_2} of alveolar gas and arterial blood to the P_{CO_2} of mixed venous blood before recirculation occurs. After recirculation, CO_2 produced by metabolism in the tissues slowly accumulates, and with cardiac output, cerebral blood flow and ventilation acting as mixers, the P_{CO_2} of the alveolar gas, arterial blood and venous blood all rise together. Since venous P_{CO_2} can be taken as a good estimate of brain P_{CO_2} during rebreathing, end-tidal P_{CO_2} during rebreathing is a measure of the input to the central chemoreceptors. Thus, rebreathing as described by Read provides a means of measuring the inputs to the central and peripheral chemoreceptors while the slowly increasing P_{CO_2} stimulates the output ventilation, and so the input–output relationship of the chemoreflexes can be determined. In this special case, central [H^+] can be estimated from arterial P_{CO_2}.

Read's method is hyperoxic, and so the ventilatory contribution of the peripheral chemoreceptors is minimised. In 1988, I introduced a rebreathing method (Duffin and McAvoy, 1988) designed to measure the input–output relations of the chemoreflexes during isoxia. In this method, the rebreathing bag initially holds the target isoxia, and oxygen is delivered to the bag to supply the oxygen consumption and maintain isoxia. Another modification was to start the rebreathing after a 5-min period of hyperventilation so that the initial equilibration was hypocapnic. As P_{CO_2} slowly increases during rebreathing, ventilation remains unchanged until P_{CO_2} reaches a ventilatory recruitment threshold, above which it increases with P_{CO_2}. This method therefore controls the peripheral and central respiratory chemoreceptor stimuli, in terms of P_{CO_2} and P_{O_2}, independent of both pulmonary gas exchange and cerebral blood flow. Using results from modified rebreathing experiments on many subjects, an average chemoreflex input–output relationship was constructed (Duffin et al., 2000). The model equations used

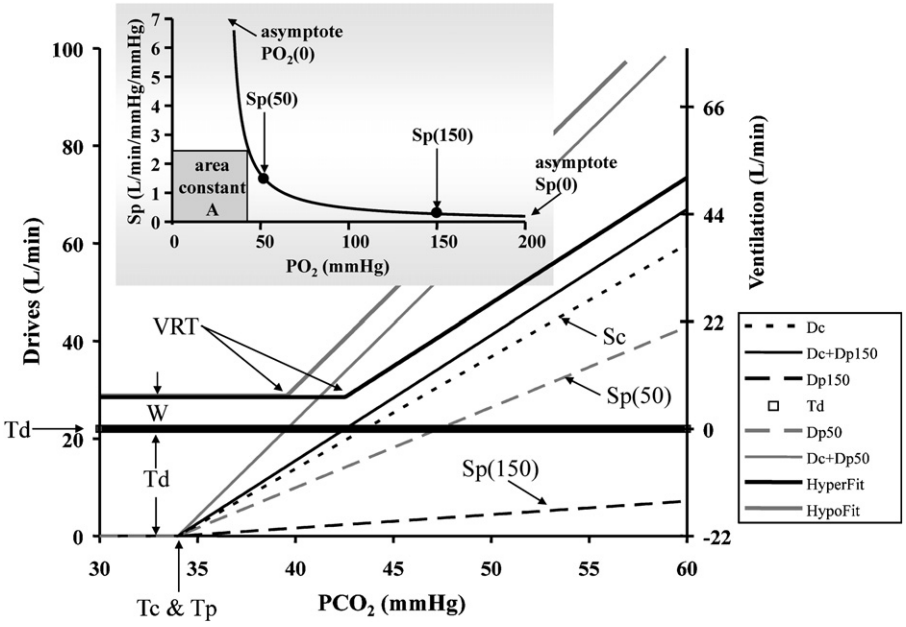

Fig. 3. The chemoreflex model equations in graphical form. The various parameters of the model are illustrated. Note that the chemoreceptor drives (left axis) do not affect ventilation (right axis) until a drive threshold is exceeded (similar to the neural activity of the carotid bodies; Torrance, 1996). The final fitted responses for hyperoxic isoxic rebreathing (HyperFit) and hypoxic isoxic rebreathing (HypoFit) are shown as thick black and grey lines respectively.

here are based on that relationship and follow the form previously published (Duffin, 2005; Duffin, 2007). They are listed in Appendix A, and should be viewed as a theoretical description of the chemoreflexes in terms of chemoreceptor drives to breathe sensitivities and thresholds that fit the current view of how the system operates; as the current view changes, so will the model.

3.5. Chemoreflex model

Fig. 3 shows the chemoreflex model equations in graphical form with the parameters labeled. The central and peripheral chemoreceptors are assigned chemoreceptor threshold P_{CO_2} tensions (Tc and Tp respectively) above which their neural activity output (chemoreflex drive) increases linearly with P_{CO_2} with slopes Sc and Sp respectively. The central slope is a constant parameter while the peripheral slope depends on P_{O_2} in a rectangular hyperbolic relationship; increasing from a low asymptotic value (Sp(0)) to a maximum at the P_{O_2} asymptote ($P_{O_2}(0)$). These drives are summed in the current model; although the assumption of additive responses has been challenged recently in dog experiments (Blain et al., 2009), those from humans (St. Croix et al., 1996) and cats (Heeringa et al., 1979) support it. However, see example subject 4 below. Ventilation is unaffected until a drive threshold (Td) is exceeded; the P_{CO_2} at which the drive exceeds the drive threshold is termed the ventilatory recruitment threshold (VRT; Mateika and Ellythy, 2003). Below the VRT, ventilation is driven by the wakefulness drive (W), which disappears during sleep.

4. The role of the central chemoreceptors

This chemoreflex model can be used to elucidate the role of the central and peripheral chemoreceptors in the steady state control of breathing for an individual. Although the results from a pair of hyperoxic and hypoxic isoxic modified rebreathing tests yield the ventilatory recruitment thresholds, and sensitivities to CO_2, they do not directly measure the chemoreceptor thresholds, the drive threshold or the parameters describing the variation of CO_2 sensitivity with P_{O_2}. And, while it is assumed that hyperoxia mimimises the peripheral response to CO_2 in most individuals so that the hyperoxic response sensitivity is the central chemoreflex sensitivity, this assumption may not apply to some individuals. However, by adjusting the parameters of the model so that the model prediction fits the results from a pair of hyperoxic and hypoxic isoxic rebreathing tests, all of the chemoreflex model parameters for an individual can be determined, including the central and peripheral chemoreceptor thresholds and whether these might be affected by acid–base factors. The model parameters reveal the variation of peripheral sensitivity to CO_2 with P_{O_2}, and the degree to which hyperoxia suppresses it, so that the true central sensitivity to CO_2 is determined. Further, the possible existence of a peripheral tonic drive to breathe can be surmised. This process therefore allows deduction of the role of the central and peripheral chemoreflexes, and acid–base factors.

It is worth noting that this process is based on the premise that the chemoreflex model is correct. Moreover, the adjustment of the model parameters to achieve a fit to rebreathing tests data requires some assumptions so that this exercise should be viewed with caution. Despite these caveats, I believe that the exercise is worth doing because it offers hypothetical explanations of how the chemoreflexes operate and the ability to predict system behavior (e.g. Duffin and Mahamed, 2003; Duffin, 2005; Duffin, 2007). While the rebreathing test results for most individuals are well fitted by the model, giving some confidence in its assumptions, as the first example below illustrates, it is when rebreathing results are not easily fitted for some individuals, so that adjustments to the model are required, that insights are gained into the variations among individuals that occur in the system operation.

The rebreathing test results examined in this way were obtained from a number of different studies that all used Duffin's modified rebreathing method; details of the conduct of such tests are given in the papers from which they were extracted. The cases shown here illustrate some of the patterns of response that may be observed, and offer the possibility of classifying rebreathing test responses according to them. Overall, they show that the central chemoreflex plays an essential role in ensuring that central $[H^+]$ is regulated despite differences in the peripheral chemoreflex between individuals, and point out that these latter possible differences should be considered when comparing responses between subjects.

Table 1
Model parameters for example subject 1.

Central		Peripheral				
Tc (mm Hg)	Sc (L/min/mm Hg)	$P_{O_2}(0)$ (mm Hg)	Sp(0) (L/min/mm Hg)	*A* (mm Hg (L/min/mm Hg))	Tp (mm Hg)	Tonic (50) (L/min)
34	2.3	30	0	33	34	0

Other						
Td (L/min)	*W*(150) (L/min)	*W*(50) (L/min)	Tp(150) (mm Hg)	Fp(150)	Tp(50) (mm Hg)	Fp(50)
22	6.5	6.8				

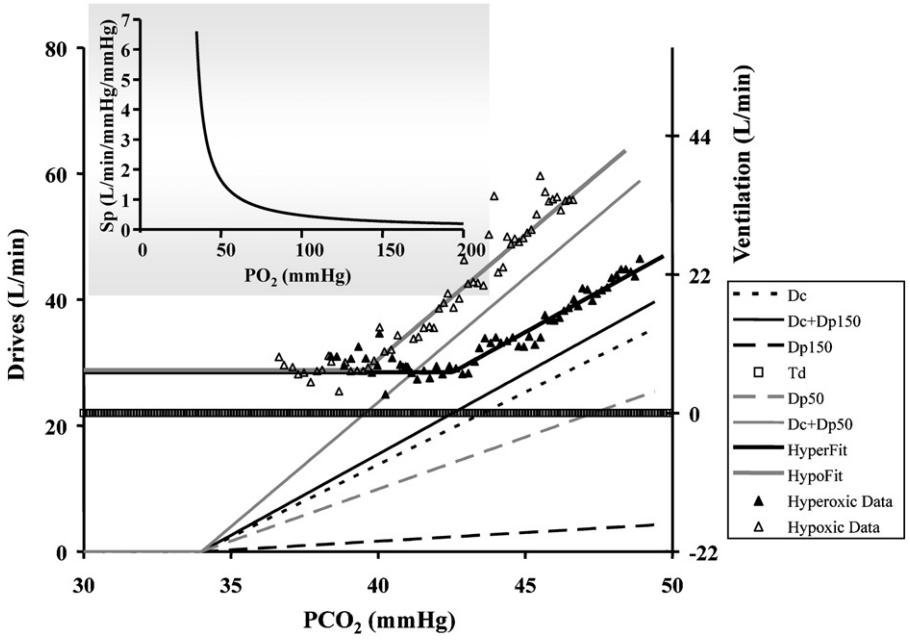

Fig. 4. A model fit to the isoxic hyperoxic (filled triangles) and hypoxic (open triangles) rebreathing responses for subject 1. These were measured at sea level for a subject that is typical of the majority. The parameters are as named in Fig. 3, and the central and peripheral drives to breathe vs. P_{CO_2} (left axis) that contribute to the fit are shown for isoxic hyperoxia (150 mm Hg) and hypoxia (50 mm Hg). The thick line at zero ventilation (right axis) is the drive threshold, which must be exceeded for the drives to affect ventilation. The r^2 values were 0.91 and 0.96 for the hyperoxic and hypoxic fits respectively.

To assist in fitting the model to the test results, the recorded breath-by-breath data for isoxic hyperoxic and hypoxic modified rebreathing tests were displayed graphically together with the model predictions; the model parameters were then adjusted until the model fitted the data with an r^2 assessment of the fit >0.8. A specially written computer program was used for this task (LabVIEW, National Instruments, Texas USA; available on request).

4.1. Example subject 1

The first set of rebreathing tests examined was measured at sea level in a sea level resident. These observations are typical of the majority of sea level subjects (e.g. Jensen et al., 2009). The responses were fitted by adjusting the model parameters to those listed in Table 1. As Fig. 4 shows, the response above the VRT is a single line with no second threshold due to changes in the pattern of breathing (confirmed by the tidal volume (VT) and frequency (*F*) responses shown in Fig. 5).

I interpreted the first example subject's chemoreflex parameters as follows. Since the peripheral and central chemoreceptor thresholds were the same, the implication is that central and peripheral acid–base conditions, and $[H^+]$ centrally and peripherally, are similar during rebreathing. The model shows that the decrease in VRT from 42.6 mm Hg in hyperoxia to 39.6 mm Hg in

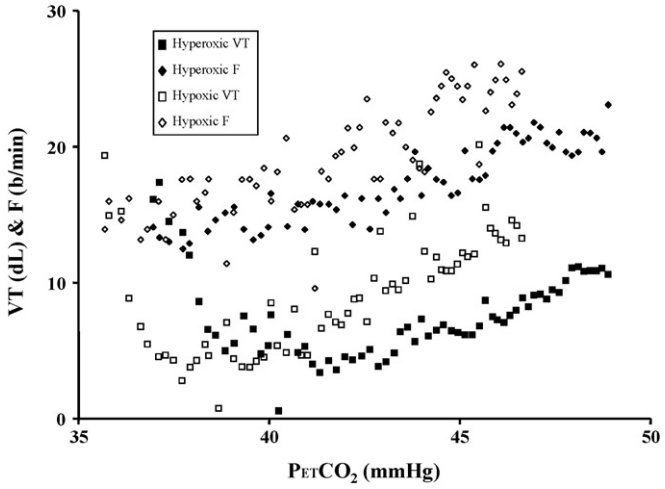

Fig. 5. The breathing pattern of subject 1. Tidal volume (VT) in decilitres and breathing frequency (*F*) in breaths/min vs. end-tidal P_{CO_2} ($P_{ET}CO_2$) for the hyperoxic (filled symbols) and hypoxic (open symbols) isoxic rebreathing tests shown in Fig. 4. Apart from the VRT, no further change in breathing pattern is discernible as $P_{ET}CO_2$ increases.

Table 2
Model parameters for example subject 2.

Central		Peripheral				
Tc (mm Hg)	Sc (L/min/mm Hg)	P_{O_2}(0) (mm Hg)	Sp(0) (L/min/mm Hg)	*A* (mm Hg (L/min/mm Hg))	Tp (mm Hg)	Tonic (50) (L/min)
20	2.2	30	0	22	20	0

Other						
Td (L/min)	*W*(150) (L/min)	*W*(50) (L/min)	Tp(150) (mm Hg)	Fp(150)	Tp(50) (mm Hg)	Fp(50)
32.8	7	7	39	2.4	33.5	3.8

hypoxia is due to the increased sensitivity of the peripheral CO_2 response with hypoxia rather than an increase in carotid body tonic activity, and that conclusion is supported by the absence of a significant increase in the basal ventilation with hypoxia (6.5–6.8 L/min). With a normal resting P_{O_2} of 100 mm Hg, resting ventilation in this individual is driven primarily by the wakefulness drive and drive from the central chemoreceptors with a sensitivity of 2.3 L/min/mm Hg, because the peripheral sensitivity to CO_2 is low at 0.28 L/min/mm Hg.

4.2. Example subject 2

The second set of rebreathing tests examined was measured in a sea level resident after acclimatisation to altitude (Slessarev et al., 2010). The responses were fitted by adjusting the model parameters as listed in Table 2. As Fig. 6 shows, the responses exhibit a second threshold above the VRT that is due to a change in the pattern of breathing (discernible in the VT and *F* responses shown in Fig. 7).

I interpreted the second example subject's chemoreflex parameters as follows. As in the first example subject, the peripheral and central chemoreceptor thresholds were the same implying that [H^+] centrally and peripherally are similar during rebreathing. However the chemoreceptor threshold P_{CO_2} tensions are reduced compared to those of the first example subject measured at sea level. If the chemoreceptor [H^+] thresholds are assumed to be unchanged from their sea level values, and acid–base conditions have compensated for the respiratory alkalosis of altitude to restore resting [H^+] to normal, then the result would be the reduced P_{CO_2} chemoreceptor thresholds observed (Duffin, 2005; Somogyi et al., 2005).

The decrease in VRT from 33.8 mm Hg in hyperoxia to 29.9 in hypoxia is due to the increased sensitivity of the peripheral CO_2 response with hypoxia rather than an increase in carotid body tonic activity, and that conclusion is supported by the absence of a significant increase in the basal ventilation with hypoxia (7.0–7.0 L/min).

In this example the second threshold is due to a change in the pattern of breathing (at P_{CO_2} tensions of 39 and 33.5 mm Hg; hyperoxic and hypoxic responses respectively) where further increases in ventilation are provided by increasing frequency as tidal volume reaches a limit of about 1.8 L as seen in Fig. 7. This patterning threshold may not be observed in a test if the increase in P_{CO_2} during the rebreathing test is restricted and tidal volume does not reach its limit, but it may become visible if ventilation is driven hard by a high P_{CO_2}.

With a resting P_{O_2} at altitude of 50 mm Hg, resting ventilation in this individual is still driven primarily by the wakefulness drive and the drive from the central chemoreceptors, although the peripheral contribution is more substantial than that in the first example subject (sensitivities to CO_2 are 2.2 and 1.1 L/min/mm Hg central and peripheral respectively).

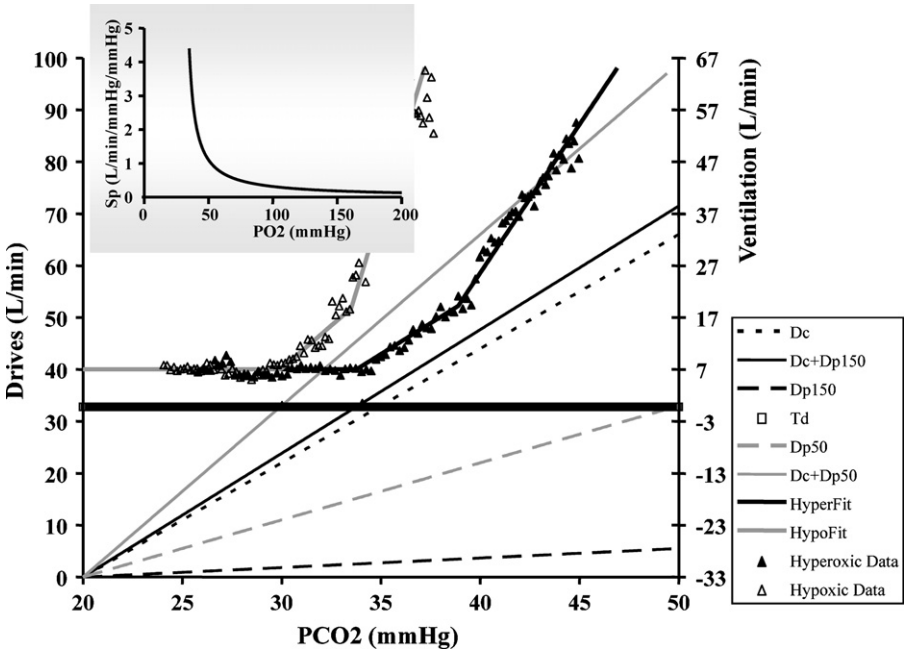

Fig. 6. A model fit to the measured isoxic hyperoxic (filled triangles) and hypoxic (open triangles) rebreathing responses for subject 2. These were measured after acclimatisation to altitude, and show a second threshold due to a change in the pattern of breathing. The parameters are as named in Fig. 3 and the central and peripheral drives to breathe vs. P_{CO_2} (left axis) that contribute to the fit are shown for isoxic hyperoxia (150 mm Hg) and hypoxia (50 mm Hg). The thick line at zero ventilation (right axis) is the drive threshold, which must be exceeded for the drives to affect ventilation. The r^2 values were 0.99 and 0.92 for the hyperoxic and hypoxic fits respectively.

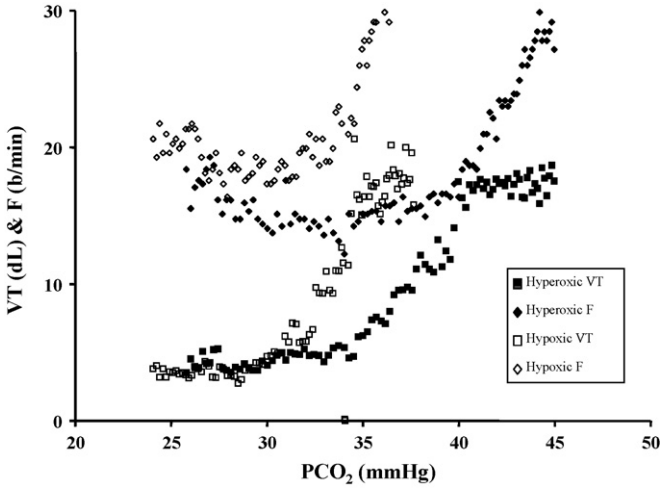

Fig. 7. The breathing pattern of subject 2. Tidal volume (VT) in decilitres and breathing frequency (F) in breaths/min vs. end-tidal P_{CO_2} (PCO_2) for the hyperoxic (filled symbols) and hypoxic (open symbols) isoxic rebreathing tests shown in Fig. 6. The breathing pattern changes as VT reaches a maximum and F increases at the patterning thresholds of 39 and 33.5 mm Hg for hyperoxic and hypoxic responses respectively.

4.3. Example subject 3

The third set of rebreathing tests examined was measured in a high altitude resident (Slessarev et al., 2010) and illustrates responses with a hypoxia-induced increase in basal ventilation and decrease in VRT. The responses were fitted by adjusting the model parameters as listed in Table 3 and illustrated in Fig. 8.

The third subject's responses showed an increase in basal ventilation and a decrease in VRT with hypoxia but little increase in slope. The latter aspect meant that the decrease in threshold was not due to the increase in slope alone, and an increase in peripheral tonic activity with hypoxia was used rather than assuming that hypoxia produced a central acidosis. The latter would change the relation between P_{CO_2} and $[H^+]$ resulting in a fall in the central chemoreceptor threshold in terms of P_{CO_2} but was assumed unlikely. The increase in the tonic drive from the peripheral chemoreceptors exceeded the drive threshold in this subject and could account for the increased basal ventilation in hypoxia.

This type of rebreathing response is typical of Andean high altitude residents (Slessarev et al., 2010), where the hypoxia-induced increase in CO_2 sensitivity is small or absent but hypoxia does produce a fall in the VRT. The presence of a tonic peripheral drive may be attributed to a change in function of the carotid body, as hypertrophy and histological changes of the carotid bodies have been observed in highlanders (Lahiri et al., 2000). This type of response is also reminiscent of those observed in the subjects studied by Nielsen and Smith (1952) that showed an increase in basal ventilation with hypoxia, albeit they used steady state methods rather than rebreathing.

Resting ventilation in this example subject is due to a combination of the wakefulness drive to breathe, a tonic peripheral drive and the central and peripheral chemoreceptor drives. With a resting P_{O_2} of 50 mm Hg the peripheral sensitivity to CO_2 is comparable to the central (0.85 vs. 1.3 L/min/mm Hg peripheral and central respectively).

4.4. Example subject 4

The final set of rebreathing tests examined was measured in a sea level resident at altitude (Slessarev et al., 2010), and illustrate responses with a second threshold above the VRT that is not due to an abrupt change in the pattern of breathing. The responses were fitted by adjusting the model parameters as listed in Table 4 and illustrated in Fig. 9, with the tidal volume and frequency responses shown in Fig. 10.

I fitted the fourth example subject's responses according to the following reasoning. First it was apparent that the second threshold

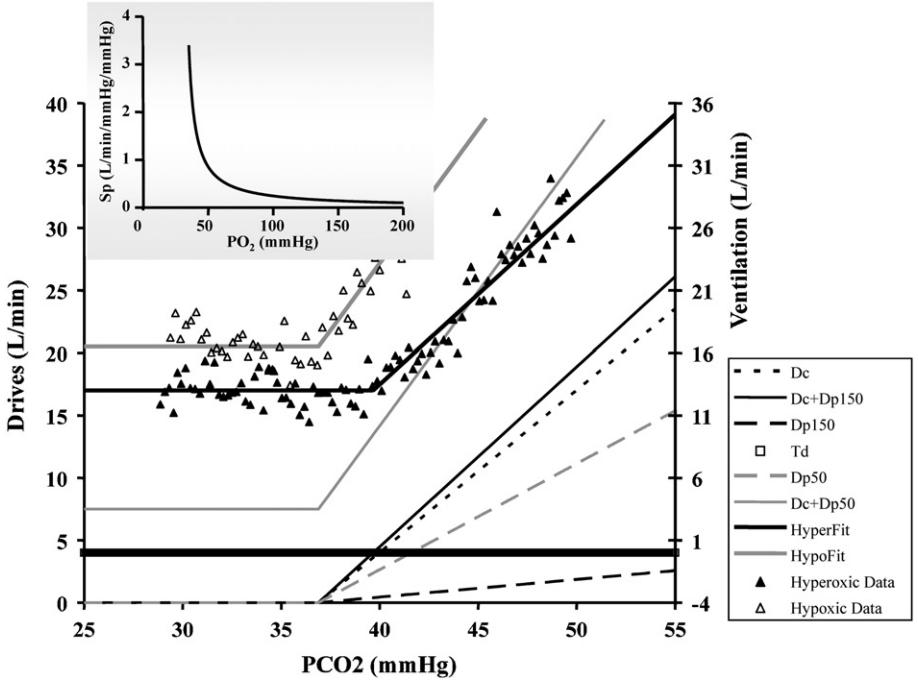

Fig. 8. A model fit to the measured isoxic hyperoxic and hypoxic rebreathing responses for subject 3. This subject displayed a hypoxia-induced increase in basal ventilation. The parameters are as shown in Fig. 3 and the central and peripheral drives to breathe vs. P_{CO_2} (left axis) that contribute to the fit are shown for isoxic hyperoxia (150 mm Hg) and hypoxia (50 mm Hg). The thick line at zero ventilation (right axis) is the drive threshold, which must be exceeded for the drives to affect ventilation. The r^2 values were 0.92 and 0.81 for the hyperoxic and hypoxic fits respectively.

Table 3
Model parameters for example subject 3.

Central		Peripheral				
Tc (mm Hg)	Sc (L/min/mm Hg)	$P_{O_2}(0)$ (mm Hg)	Sp(0) (L/min/mm Hg)	*A* (mm Hg (L/min/mm Hg))	Tp (mm Hg)	Tonic (50) (L/min)
36.9	1.3	30	0	17	36.9	7.5

Other						
Td (L/min)	*W*(150) (L/min)	*W*(50) (L/min)	Tp(150) (mm Hg)	Fp(150)	Tp(50) (mm Hg)	Fp(50)
4	13	13				

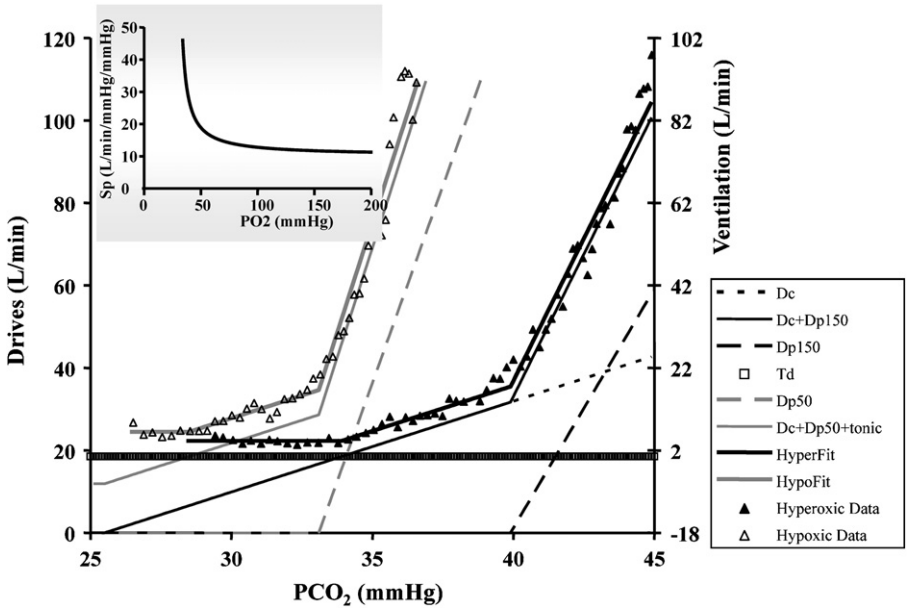

Fig. 9. A model fit to the measured isoxic hyperoxic and hypoxic rebreathing responses for subject 4. This subject displayed a second threshold, which was not due to an abrupt change in the pattern of breathing. The parameters are as named in Fig. 3, and the central and peripheral drives to breathe vs. P_{CO_2} (left axis) that contribute to the fit are shown for isoxic hyperoxia (150 mmHg) and hypoxia (50 mmHg). The thick line at zero ventilation (right axis) is the drive threshold, which must be exceeded for the drives to affect ventilation. The r^2 values were 0.99 and 0.92 for the hyperoxic and hypoxic fits respectively.

was not due to a change in the pattern of breathing after examining the VT and *F* responses. Second, since there was a change in slope with hypoxia above the second threshold but not below, it was assumed that the second threshold was due to the appearance of the peripheral drive to breathe. Moreover the contribution was considerable even in hyperoxia because the slope increased above the second threshold. The difference in the second slopes between hyperoxic and hypoxic responses is set by parameter *A* in the Sp vs. P_{O_2} relationship and although parameter *A* also affects the Sp(150) its adjustment was insufficient in this case to account for the hyperoxic peripheral response and so the asymptote parameter Sp(0) was not zero as is usually assumed.

The difference between central and peripheral chemoreceptor thresholds could result from either a difference in their respective [H^+] thresholds or a difference in the acid–base conditions so that the P_{CO_2} thresholds differed but the [H^+] thresholds were the same. These possibilities cannot be distinguished, but given the unusual peripheral response and the large difference in P_{CO_2} thresholds, the former possibility seems likely. The model must also account for the decrease in both the VRT and the second threshold with hypoxia. The decrease in VRT is not due to the change in the peripheral response slope in this case and was assumed to be due to an increase in the tonic activity of the peripheral chemoreceptors. An alternative assumption is that there is a change in central acid–base conditions such as a hypoxia-induced lactic acidosis so that the central chemoreceptor P_{CO_2} threshold decreased without a change in the central [H^+] threshold. This assumption seems unlikely given the enhanced peripheral response already noted, but cannot be distinguished from the observed responses, although the increase in the wakefulness parameter from 4.3 L/min in hyperoxia to 6.5 L/min in hypoxia supports the idea of a tonic peripheral drive. The decrease in the second threshold was mod-

Table 4
Model parameters for example subject 4.

Central Tc (mm Hg)	Sc (L/min/mm Hg)	Peripheral $P_{O_2}(0)$ (mm Hg)	Sp(0) (L/min/mm Hg)	*A* (mm Hg (L/min/mm Hg))	Tp (mm Hg)	Tonic (50) (L/min)
25.5	2.2	30	10.1	180	39.9/33.1	11.9

Other						
Td (L/min)	*W*(150) (L/min)	*W*(50) (L/min)	Tp(150) (mm Hg)	Fp(150)	Tp(50) (mm Hg)	Fp(50)
18.5	4.3	6.5				

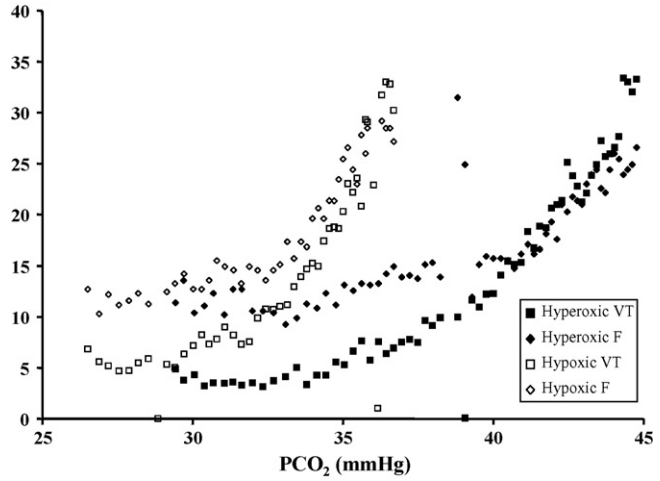

Fig. 10. The breathing pattern of subject 4. Tidal volume (VT) in decilitres and breathing frequency (F) in breaths/min vs. end-tidal P_{CO_2} (PCO_2) for the hyperoxic (filled symbols) and hypoxic (open symbols) isoxic rebreathing tests shown in Fig. 9. The breathing pattern changes at the patterning thresholds of 39 and 33.5 mmHg for hyperoxic and hypoxic responses respectively, but no abrupt changes in the VT and F responses are discernible, apart from the VRT.

eled by decreasing the peripheral threshold from 39.9 mm Hg in hyperoxia to 33.1 mm Hg in hypoxia; an unusual change in terms of its rapidity, but one that has been postulated to occur during adaptation to hypoxia (Duffin and Mahamed, 2003).

In summary, this type of response is observed infrequently and may indicate a subject with a highly responsive peripheral chemoreflex, possibly with a peripheral chemoreceptor threshold higher than that of the central chemoreceptors. In such subjects the resting ventilation might be due entirely to the wakefulness and central chemoreflex drives to breathe, and hyperoxia may not silence the peripheral response to CO_2. With such a high response to hypoxia, perhaps their peripheral responses differ from most and should be modeled as shown in Fig. 11 (Table 5).

In this alternative model the main difference is that the peripheral response does not add to the central response but acts as a multiplier, altering the sensitivity of the central response. The chemoreceptor thresholds are similar to the previous additive interaction model and again the peripheral thresholds are higher than the central threshold, with a tonic peripheral drive during hypoxia used to account for the shift in the VRT as before. This model has the advantage of providing a curvilinear response, rather than a straight line, which might fit this particular data better, and raises the question as to whether the central–peripheral interaction in some individuals might be multiplicative in contrast to the additive interaction and linear responses in most.

5. A dynamic simulation of the respiratory control system

To further examine the role of the central chemoreceptors I constructed a dynamic model of the respiratory control system so that the effect of different chemoreflex characteristics, and in particular the central chemoreflex, could be observed in a model simulation. First, the chemoreflex model was incorporated into a steady state model of the respiratory control system as described in previous papers (Duffin, 2005; Duffin, 2007; Ainslie and Duffin, 2009). Two factors were taken into account.

5.1. Cerebrovascular reactivity

The first factor was the effect of cerebrovascular reactivity. In contrast to the modified rebreathing test conditions where arterial to tissue differences are minimized so that central and peripheral P_{CO_2} values are similar; in an intact individual, central chemoreceptor P_{CO_2} differs from arterial P_{CO_2} so that the central and peripheral chemoreceptor thresholds also differ, with the central P_{CO_2} higher than the arterial and the central chemoreceptor threshold correspondingly displaced downward. This displacement is affected by the CO_2 production of medullary tissue and the medullary blood flow as explained earlier. Cerebral blood flow control therefore participates in mitigating the effects of changing arterial P_{CO_2} on

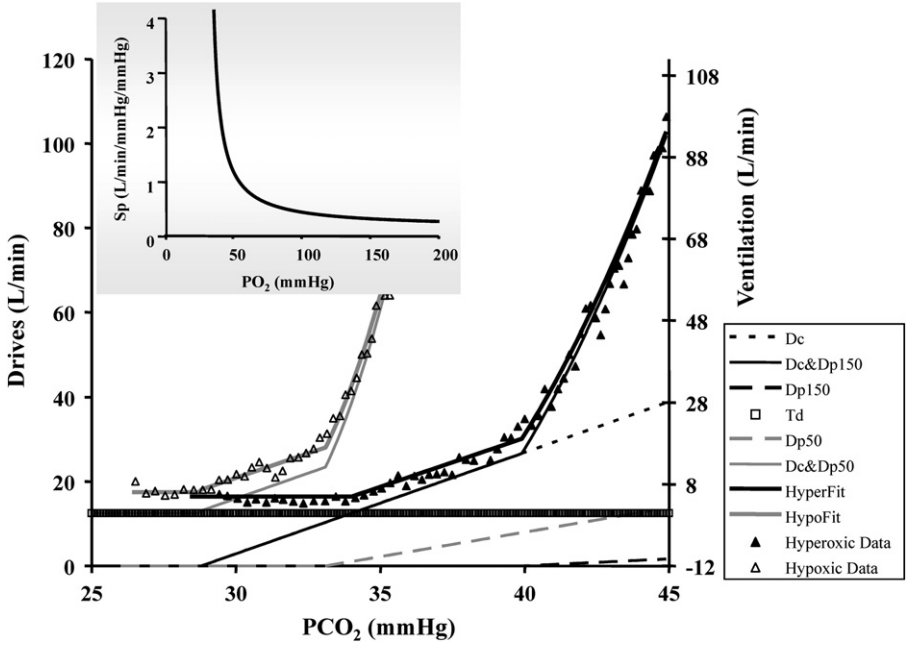

Fig. 11. An alternative model fit to the measured isoxic hyperoxic and hypoxic rebreathing responses for subject 4. The parameters are as named in Fig. 3, and the central and peripheral drives to breathe vs. P_{CO_2} (left axis) that contribute to the fit are shown for isoxic hyperoxia (150 mm Hg) and hypoxia (50 mm Hg). The thick line at zero ventilation (right axis) is the drive threshold, which must be exceeded for the drives to affect ventilation. The r^2 values were 0.961 and 0.895 for the hyperoxic and hypoxic fits respectively.

Table 5
Alternative model parameters for example subject 4.

Central		Peripheral				
Tc (mm Hg)	Sc (L/min/mm Hg)	$P_{O_2}(0)$ (mm Hg)	Sp(0) (L/min/mm Hg)	A (mm Hg (L/min/mm Hg))	Tp (mm Hg)	Tonic (50) (L/min)
28.8	2.4	30	0.16	20	39.9/33.1	13.1

Other						
Td (L/min)	W(150) (L/min)	W(50) (L/min)	Tp(150) (mm Hg)	Fp(150)	Tp(50) (mm Hg)	Fp(50)
12.5	5	6.1				

central P_{CO_2}, thereby defending central [H^+]. The cerebral blood flow model used here was described in Ainslie and Duffin (2009) and is stated in Appendix A. It assumes that the cerebral vasculature responds to its local P_{CO_2} and P_{O_2}, with arterial P_{CO_2} assumed to be a major factor (Ide et al., 2003). However, it must be emphasized that this assumption is a simplification of the complex control of cerebrovascular reactivity that is yet to be fully understood (e.g. Fan et al., 2010).

5.2. Interaction of cerebrovascular reactivity and the chemoreflexes

Fig. 12 shows a graphical model of the steady state for example subject 1. It incorporates the iso-metabolic hyperbola describing the forward part of the control loop and the chemoreflexes forming the feedback part, and shows the response to CO_2 in hyperoxia that would be observed during rebreathing as well as the actual response that incorporates the effect of cerebral blood flow that would be observed in steady state tests. This steady state model shows that as cerebrovascular reactivity increases, the arterial to central P_{CO_2} difference decreases and the slope of the ventilation response declines (Berkenbosch et al., 1989; Mohan et al., 1999). The intersection of the iso-metabolic hyperbola with the steady state responses is the system resting equilibrium point defining the resting ventilation and P_{CO_2}.

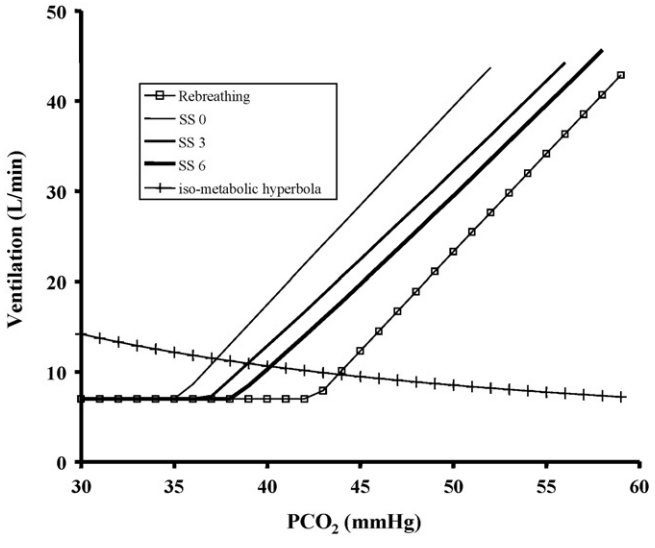

Fig. 12. A model of the steady state isoxic hyperoxic response to CO_2 for subject 1. Here showing the responses that would be observed with a modified rebreathing test and those that would be observed by steady state testing (SS) where cerebral blood flow affects the arterial to central (brain) P_{CO_2} difference. The cerebrovascular reactivity model used was that stated in Appendix A with the following parameters: Qn = 75, $P_{CO_2 n} = 30$ and sensitivities of 0, 3 and 6 (SS 0, SS 3 and SS 6).

5.3. Acid–base balance

The second factor involves the translation of P_{CO_2} into the [H^+] stimulus of the chemoreceptors. The model of acid–base relations I used is based on the physicochemical approach introduced by Stewart (Stewart, 1983). In Stewart's approach, P_{CO_2} and two other variables, SID (strong ion difference; the concentration difference of strongly dissociated positive and negative ions in solution) and [A_{tot}] (the total concentration of weakly dissociated anions in solution) are the independent variables that determine the dependent variables [H^+] and [HCO_3^-]. This model has been updated to consider the concentration of weakly dissociated anions in plasma in more detail, with phosphate and albumin concentrations substituted for [A_{tot}] (Watson, 1999). Its incorporation into a model of the chemoreflexes based on [H^+] inputs to the chemoreceptors takes the same form as the model listed in Appendix A and is fully described in Duffin (2005).

The dynamic model including cerebral blood flow control by arterial [H^+] and chemoreceptor stimuli in terms of [H^+] was constructed with a simple 3-compartment model of lungs, brain and other tissues as shown in Fig. 1. It was simulated using a graphical programming language (LabVIEW, National Instruments, Texas USA; program available on request) to solve the resulting mass balance equations with Euler integration, and display the dynamic changes in several respiratory variables in a manner similar to an experimental data acquisition system. The model subject characteristics such as oxygen consumption can be set, as can the chemoreflex and cerebral blood flow control parameters and acid–base factors. While the simulation is running it can be paused to allow the application of challenges such as changes in inspired gases or changes in the parameter settings. Switches to remove the wakefulness drive (sleep) or hyperventilate (sigh) are also provided.

5.4. System stability

Two experiments were done using the dynamic model to illustrate the role of the central chemoreceptors. The model chemoreflex parameters were set to those of experimental subject 2 who was acclimatized to altitude, with the wakefulness drive at zero to simulate sleep. The first experiment shows how a decrease in the central chemoreflex CO_2 sensitivity to half its normal value produces a rise in central P_{CO_2} and induces unstable periodic or Cheyne–Stokes breathing, but doubling the cerebrovascular reactivity increases the central P_{CO_2} further and damps the respiratory oscillations. This experiment is shown in Fig. 13.

The second experiment showed how, with a cerebrovascular reactivity halved, a sigh transformed a stable breathing pattern into a periodic or Cheyne–Stokes one, but restoring the cerebrovascular reactivity to normal also restored stability. The experiment is shown in Fig. 14.

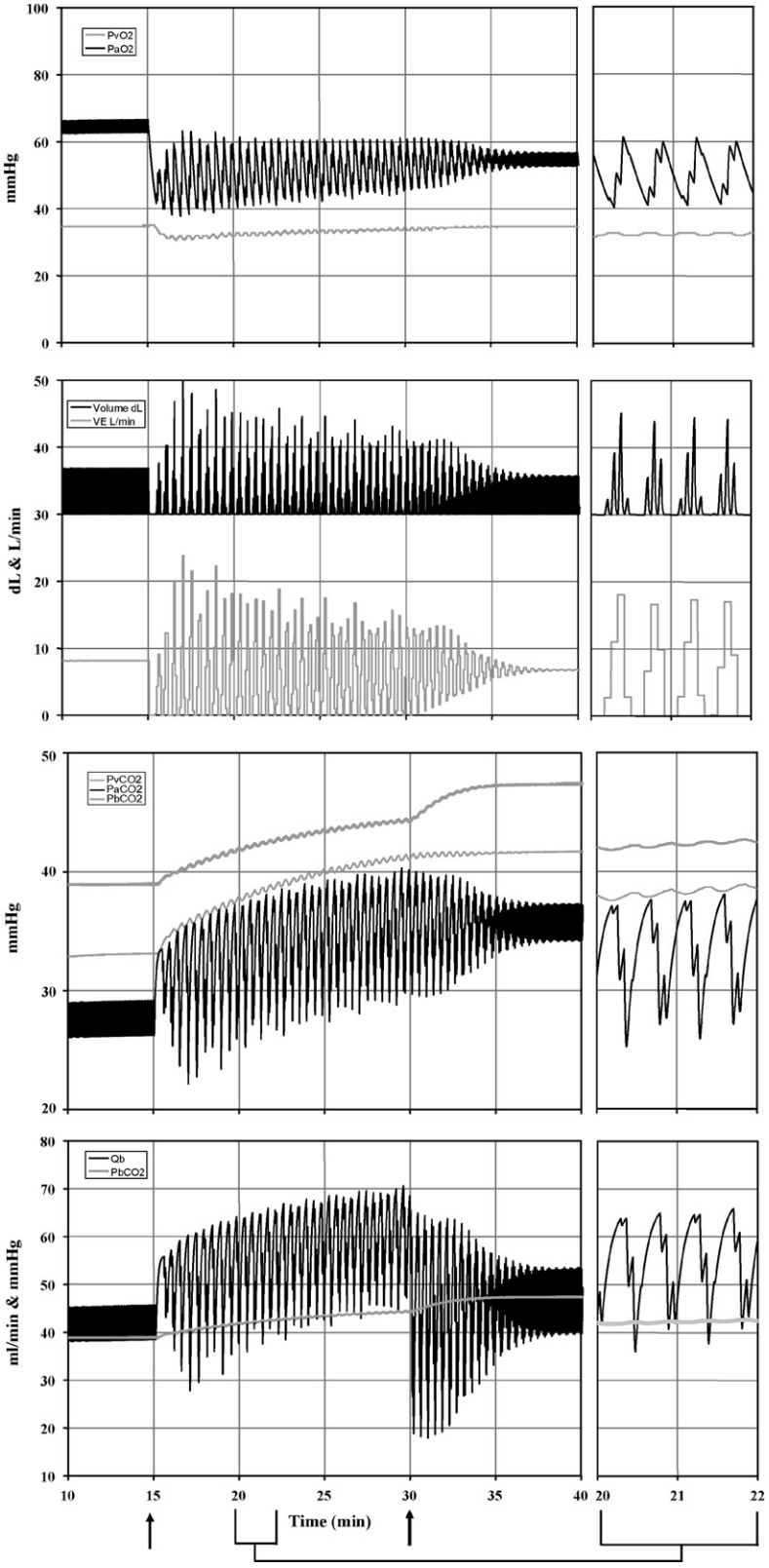

Fig. 13. A screenshot of the dynamic simulation model panel for experimental subject 2. Here the model is for sleeping at altitude (FIO_2 = 14%). The top graph shows the venous and arterial P_{O_2} (mm Hg) vs. time (min), the second graph shows the lung volume (dL) and ventilation (L/min) vs. time (min), the third graph shows the venous, arterial and brain (central) P_{CO_2} (mm Hg) vs. time (min), and the lowest graph shows the cerebral (brain) blood flow (CBF ml/min) and brain (central) P_{CO_2} (mm Hg) vs. time (min). The graphs at the right show a time-expanded view between 20 and 22 min to illustrate the pattern of instability. Breathing is stable until the central chemoreflex sensitivity is reduced from 2.2 to 1.1 L/min/mm Hg at the first arrow, and then it becomes unstable as brain blood flow and P_{CO_2} increase. Breathing is then stabilized again by doubling the cerebrovascular reactivity at the second arrow, which causes a decrease in brain blood flow and an increase in brain P_{CO_2}, restoring the dominance of the central drive to breathe and stabilizing the breathing pattern.

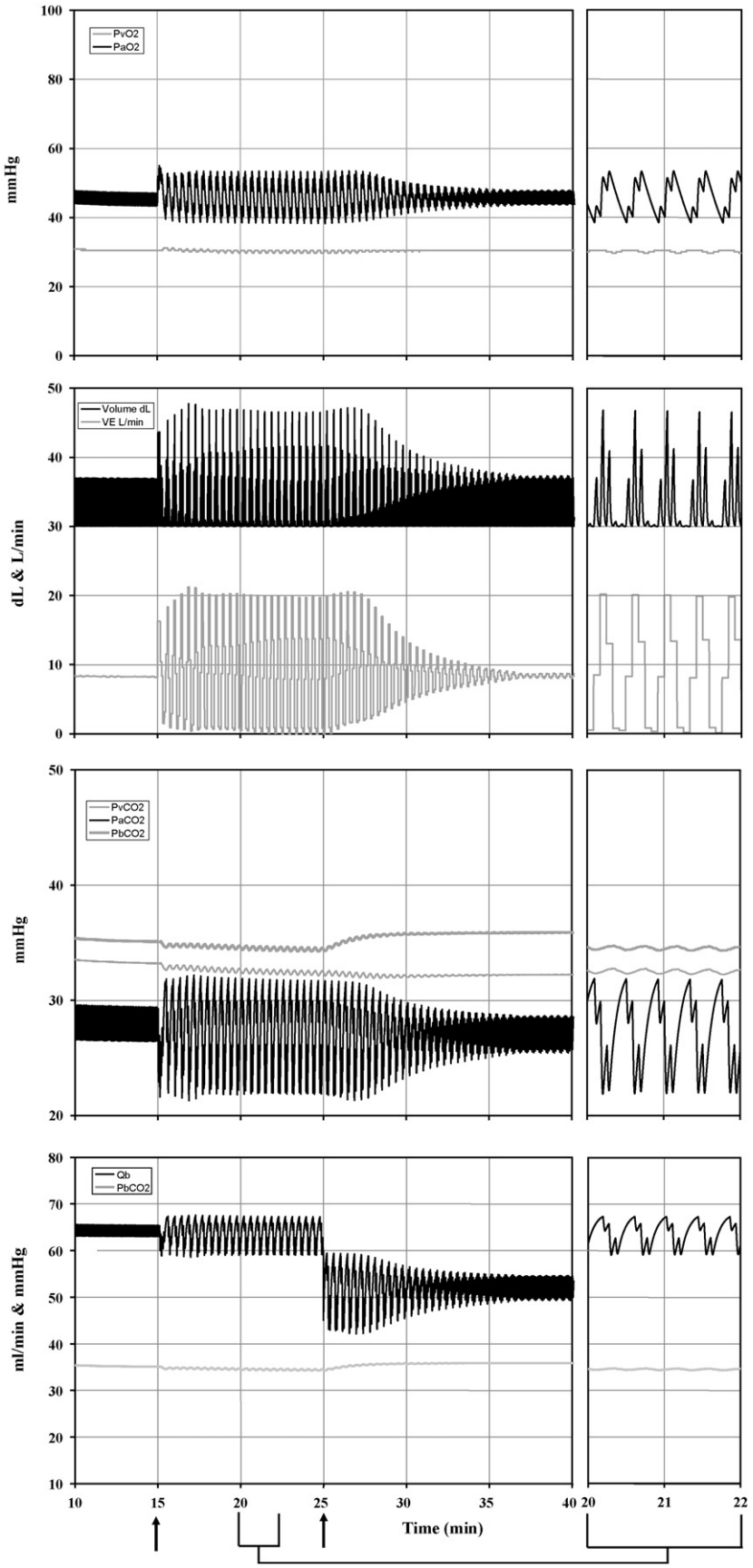

Fig. 14. A screenshot of the dynamic simulation model panel for experimental subject 2. Here the model is for sleeping at altitude (FIO_2 = 12%) with cerebrovascular reactivity half normal. The graphs are as described in Fig. 12. A sigh at the first arrow transforms the breathing pattern into an unstable one, but restoration of the cerebrovascular reactivity to normal at the second arrow lowers the brain blood flow and raises central P_{CO_2}, restoring the dominance of the central drive to breathe and stabilizing the breathing pattern.

6. Conclusion

The modeling experiments chosen here illustrate the major role played by the central chemoreceptors, not only in supporting ventilation at rest but also in stabilizing breathing in situations like sleeping at altitude where other factors may combine to alter the central chemoreceptor environment and reduce stability. Challenging the current model of the respiratory chemoreflexes to explain and predict the experimental findings from modified rebreathing tests not only provides insight into the role of the central chemoreceptors but also into the assumptions of the model itself, showing that certain peripheral chemoreceptor characteristics differ among individuals and require further experimental examination.

Acknowledgement

My thanks are extended to all at Thornhill Research and in particular to Dr. Joseph Fisher for encouraging and supporting this work.

Appendix A. Chemoreflex model equations

A.1. Rectangular hyperbolic relation between peripheral sensitivity to P_{CO_2} (Sp) and P_{O_2}

$$\mathrm{Sp} = \mathrm{Sp}(0) + \frac{A}{P_{O_2} - P_{O_2}(0))} \tag{1}$$

where Sp is the peripheral chemoreceptor sensitivity to P_{CO_2} (L/min/mm Hg); Sp(0) is the rectangular hyperbola asymptote for Sp (L/min/mm Hg); $P_{O_2}(0)$ is the rectangular hyperbola asmyptote for P_{O_2} (mm Hg) and A is the rectangular hyperbola area constant (mm Hg L/min/mm Hg).

A.2. Linear relation between peripheral drive to breathe and P_{CO_2}

$$\begin{aligned} &\text{if}(P_{CO_2} - \mathrm{Tp} > 0) \\ &\quad \mathrm{Dp} = \mathrm{Sp} \times (P_{CO_2} - \mathrm{Tp}) + \text{tonic}; \\ &\text{else } \mathrm{Dp} = \text{tonic} \end{aligned} \tag{2}$$

where Dp is the peripheral chemoreceptor drive to breathe (L/min); Tp is the peripheral chemoreceptor threshold for P_{CO_2} (mm Hg) and tonic is the peripheral drive independent of CO_2.

A.3. Linear relation between central drive to breathe and P_{CO_2}

$$\begin{aligned} &\text{if}(P_{CO_2} - \mathrm{Tc} > 0) \\ &\quad \mathrm{Dc} = \mathrm{Sc} \times (P_{CO_2} - \mathrm{Tc}); \\ &\text{else } \mathrm{Dc} = 0 \end{aligned} \tag{3}$$

where Dc is the central chemoreceptor drive to breathe (L/min); Sc is the central chemoreceptor sensitivity to P_{CO_2} (L/min/mm Hg) and Tc is the central chemoreceptor threshold for P_{CO_2} (mm Hg).

A.4. Patterning the ventilation response to P_{CO_2} and P_{O_2}

$$\begin{aligned} &\text{if}(\mathrm{Dp} + \mathrm{Dc} > \mathrm{Td}) \\ &\mathrm{DVE} = (\mathrm{Dp} + \mathrm{Dc}) - \mathrm{Td} + W; \\ &\text{else } \mathrm{DVE} = W \end{aligned} \tag{4}$$

where DVE is the ventilation drive (L/min); Td is the chemoreflex drive threshold (L/min) and W is the wakefulness drive to breathe (L/min).

$$\begin{aligned} &\text{if}(\mathrm{DVE} > \mathrm{TP}) \\ &\mathrm{VE} = \mathrm{FP} \times \mathrm{DVE}; \\ &\text{else } \mathrm{VE} = \mathrm{DVE} \end{aligned} \tag{5}$$

where VE is the ventilation (L/min); TP is the patterning threshold (mm Hg) and FP is the slope proportionality constant.

A.5. Brain compartment equation

$$Pb_{CO_2} - Pa_{CO_2} = \frac{V_{CO_2}}{K \times Q} \tag{6}$$

where Pb_{CO_2} is the brain or central P_{CO_2} (mm Hg); Pa_{CO_2} is the arterial P_{CO_2} (40 mm Hg at rest); V_{CO_2} is central CO_2 production (3 ml/min per 100 g at rest); Q is the central blood flow (55 ml/min per 100 g at rest) and K is the slope of the linearized CO_2 dissociation curve (0.005 ml/ml/mm Hg).

A.6. Cerebrovascular reactivity

$$Q = \mathrm{Qr} + \mathrm{Qs}(Pa_{CO_2} - Pr_{CO_2}) \tag{7}$$

where Qr is the resting central blood flow (55 ml/min per 100 g); Qs is the central blood flow sensitivity (2 ml/min per 100 g per mm Hg) and Pr_{CO_2} is the resting Pa_{CO_2}.

A.7. Cerebral blood flow and central (brain) P_{CO_2}

$$Pb_{CO_2} = \frac{Pa_{CO_2} + V_{CO_2}}{K(\mathrm{Qr} + \mathrm{Qs}(Pa_{CO_2} - Pr_{CO_2}))} \tag{8}$$

References

Ainslie, P.N., Duffin, J., 2009. Integration of cerebrovascular CO_2 reactivity and chemoreflex control of breathing: mechanisms of regulation, measurement, and interpretation. Am. J. Physiol. Regul. Integr. Comp. Physiol. 296, R1473–R1495.

Bell, H.J., 2006. Respiratory control at exercise onset: an integrated systems perspective. Respir. Physiol. Neurobiol. 152, 1–15.

Berkenbosch, A., Bovill, J.G., Dahan, A., DeGoede, J., Olievier, I.C., 1989. The ventilatory CO_2 sensitivities from Read's rebreathing method and the steady-state method are not equal in man. J. Physiol. 411, 367–377.

Blain, G.M., Smith, C.A., Henderson, K.S., Dempsey, J.A., 2009. Contribution of the carotid body chemoreceptors to eupneic ventilation in the intact, unanesthetized dog. J. Appl. Physiol. 106, 1564–1573.

Corcoran, A.E., Hodges, M.R., Wu, Y., Wang, W., Wylie, C.J., Deneris, E.S., Richerson, G.B., 2009. Medullary serotonin neurons and central CO_2 chemoreception. Respir. Physiol. Neurobiol. 168, 49–58.

Dahan, A., Nieuwenhuijs, D., Teppema, L., 2007. Plasticity of central chemoreceptors: effect of bilateral carotid body resection on central CO_2 sensitivity. PLoS Med. 4, e239.

Duffin, J., 2005. Role of acid–base balance in the chemoreflex control of breathing. J. Appl. Physiol. 99, 2255–2265.

Duffin, J., 2007. Measuring the ventilatory response to hypoxia. J. Physiol. 584, 285–293.

Duffin, J., Mahamed, S., 2003. Adaptation in the respiratory control system. Can. J. Physiol. Pharmacol. 81, 765–773.

Duffin, J., McAvoy, G.V., 1988. The peripheral-chemoreceptor threshold to carbon dioxide in man. J. Physiol. 406, 15–26.

Duffin, J., Mohan, R.M., Vasiliou, P., Stephenson, R., Mahamed, S., 2000. A model of the chemoreflex control of breathing in humans: model parameters measurement. Respir. Physiol. 120, 13–26.

Farhi, L.E., Rahn, H., 1960. Dynamics of changes in carbon dioxide stores. Anesthesiology 21, 604–614.

Fan, J.-L., Burgess, K.R., Basnyat, R., Thomas, K.N., Peebles, K.C., Lucas, S.J.E., Lucas, R.A.I., Donnelly, J., Cotter, J.D., Ainslie, P.N., 2010. Influence of high altitude on cerebrovascular and ventilatory responsiveness to CO_2. J. Physiol. 588, 539–549.

Fink, B.R., 1961. Influence of cerebral activity in wakefulness on regulation of breathing. J. Appl. Physiol. 16, 15–20.

Guyenet, P.G., Bayliss, D.A., Stornetta, R.L., Fortuna, M.G., Abbott, S.B.G., DePuy, S.D., 2009. Retrotrapezoid nucleus, respiratory chemosensitivity and breathing automaticity. Respir. Physiol. Neurobiol. 168, 59–68.

Heeringa, J., Berkenbosch, A., De Goede, J., Olievier, C.N., 1979. Relative contribution of central and peripheral chemoreceptors to the ventilatory response to CO_2 during hyperoxia. Respir. Physiol. 37, 365–379.
Ide, K., Eliasziw, M., Poulin, M.J., 2003. Relationship between middle cerebral artery blood velocity and end-tidal PCO_2 in the hypocapnic–hypercapnic range in humans. J. Appl. Physiol. 95, 129–137.
Iturriaga, R., Varas, R., Alcayaga, J., 2007. Electrical and pharmacological properties of petrosal ganglion neurons that innervate the carotid body. Respir. Physiol. Neurobiol. 157, 130–139.
Jensen, D., Mask, G., Tschakovsky, M.E., 2009. Variability of the ventilatory response to Duffin's modified hyperoxic and hypoxic rebreathing procedure in healthy awake humans. Respir. Physiol. Neurobiol. 170, 185–197.
Jounieaux, V., Parreira, V.F., Aubert, G., Dury, M., Delguste, P., Rodenstein, D.O., 2002. Effects of hypocapnic hyperventilation on the response to hypoxia in normal subjects receiving intermittent positive-pressure ventilation. Chest 121, 1141–1148.
Kumar, P., 2007. Sensing hypoxia in the carotid body: from stimulus to response. Essays Biochem. 43, 43–60.
Lahiri, S., Rozanov, C., Cherniack, N.S., 2000. Altered structure and function of the carotid body at high altitude and associated chemoreflexes. High Alt. Med. Biol. 1, 63–74.
Longobardo, G.S., Evangelisti, C.J., Cherniack, N.S., 2008. Analysis of the interplay between neurochemical control of respiration and upper airway mechanics producing upper airway obstruction during sleep in humans. Exp. Physiol. 93, 271–287.
Lopez-Barneo, J., Ortega-Saenz, P., Pardal, R., Pascual, A., Piruat, J.I., Duran, R., Gomez-Diaz, R., 2009. Oxygen sensing in the carotid body. Ann. N. Y. Acad. Sci. 1177, 119–131.
Mateika, J.H., Duffin, J., 1995. A review of the control of breathing during exercise. Eur. J. Appl. Physiol. 71, 1–27.
Mateika, J.H., Ellythy, M., 2003. Chemoreflex control of ventilation is altered during wakefulness in humans with OSA. Respir. Physiol. Neurobiol. 138, 45–57.
Mohan, R., Duffin, J., 1997. The effect of hypoxia on the ventilatory response to carbon dioxide in man. Respir. Physiol. 108, 101–115.
Mohan, R.M., Amara, C.E., Cunningham, D.A., Duffin, J., 1999. Measuring the central-chemoreflex sensitivity in man: rebreathing and steady-state methods compared. Respir. Physiol. 115, 23–33.
Nattie, E., Li, A., 2009. Central chemoreception is a complex system function that involves multiple brain stem sites. J. Appl. Physiol. 106, 1464–1466.
Nattie, E.E., 1990. The alphastat hypothesis in respiratory control and acid–base balance. J. Appl. Physiol. 69, 1201–1207.
Nielsen, M., Smith, H., 1952. Studies on the regulation of respiration in acute hypoxia. Acta Physiol. Scand. 24, 293–313.
Okada, Y., Chen, Z.B., Jiang, W.H., Kuwana, S.I., Eldridge, F.L., 2002. Anatomical arrangement of hypercapnia-activated cells in the superficial ventral medulla of rats. J. Appl. Physiol. 2, 427–439.
Orem, J., Lovering, A.T., Dunin-Barkowski, W., Vidruk, E.H., 2002. Tonic activity in the respiratory system in wakefulness, NREM and REM sleep. Sleep 25, 488–496.
Putnam, R.W., Filosa, J.A., Ritucci, N.A., 2004. Cellular mechanisms involved in CO(2) and acid signaling in chemosensitive neurons. Am. J. Physiol. Cell Physiol. 287, C1493–C1526.
Read, D.J.C., 1967. A clinical method for assessing the ventilatory response to CO_2. Aust. Ann. Med. 16, 20–32.
Shea, S.A., 1996. Behavioural and arousal-related influences on breathing in humans. Exp. Physiol. 81, 1–26.
Slessarev, M., Mardimae, A., Preiss, D., Vesely, A., Balaban, D., Greene, R., Duffin, J., Fisher, J.A., 2010. Differences in the control of breathing between Andean highlanders and lowlanders after 10-days acclimatization at 3,850 m. J. Physiol., in press.
Somogyi, R.B., Preiss, D., Vesely, A., Fisher, J.A., Duffin, J., 2005. Changes in respiratory control after 5 days at altitude. Respir. Physiol. Neurobiol. 145, 41–52.
St. Croix, C.M., Cunningham, D.A., Paterson, D.H., 1996. Nature of the interaction between central and peripheral chemoreceptor drives in human subjects. Can. J. Physiol. Pharmacol. 74, 640–646.
Stephenson, R., 2004. A theoretical study of the effect of circadian rhythms on sleep-induced periodic breathing and apnoea. Respir. Physiol. Neurobiol. 139, 303–319.
Stewart, P.A., 1983. Modern quantitative acid–base chemistry. Can. J. Physiol. Pharmacol. 61, 1444–1461.
Stuhmiller, J.H., Stuhmiller, L.M., 2005. A mathematical model of ventilation response to inhaled carbon monoxide. J. Appl. Physiol. 98, 2033–2044.
Topor, Z.L., Vasilakos, K., Younes, M., Remmers, J.E., 2007. Model based analysis of sleep disordered breathing in congestive heart failure. Respir. Physiol. Neurobiol. 155, 82–92.
Torrance, R.W., 1996. Prolegomena. Chemoreception upstream of transmitters. In: Zapata (Ed.), Frontiers in Arterial Chemoreception, vol. 410. Plenum Press, New York, pp. 13–38.
Ursino, M., Magosso, E., 2004. Interaction among humoral and neurogenic mechanisms in ventilation control during exercise. Ann. Biomed. Eng. 32, 1286–1299.
Watson, P.D., 1999. Modeling the effects of proteins on pH in plasma. J. Appl. Physiol. 86, 1421–1427.
Wolf, M.B., Garner, R.P., 2007. A mathematical model of human respiration at altitude. Ann. Biomed. Eng. 35, 2003–2022.
Zhou, H., Saidel, G.M., Cabrera, M.E., 2007. Multi-organ system model of O_2 and CO_2 transport during isocapnic and poikilocapnic hypoxia. Respir. Physiol. Neurobiol. 156, 320–330.